CrossMark

EXPERT REVIEW

# Dose optimization: a review of CT imaging for PET attenuation correction

Samuel L. Brady[1] · Barry L. Shulkin[1]

## Abstract

*Purpose* Review limitations and benefits of various options for CT-based attenuation correction for PET/CT studies.

*Methods* With the combination of PET and CT, came the combination of patient radiation dose from the two imaging modalities. Modern advances in CT technology provide opportunities to design CT acquisitions for attenuation correction allowing for the optimization of the attenuation correction acquisition for specific clinical purposes. We reviewed published literature, accepted practices, and the authors' experience, to identify and classify various tailored approaches for CT attenuation correction of PET emission data.

*Results* ImageWisely recommends three broad categories for dose optimization of attenuation correction in PET/CT imaging: (1) attenuation correction at diagnostic CT quality (PET/CTD); (2) attenuation correction for anatomic localization only of PET images (PET/CTAL); and (3) for PET attenuation correction only (PET/CTAC). The advantages, disadvantages, and dosimetry for each approach are considered.

*Conclusions* Modern dose reduction techniques allow some CTAL and CTAC exams to have a sufficient image quality for anatomic localization at radiation dose levels equivalent to the previous radionuclide attenuation correction method with [68-Ge/68-Ga] transmission sources. Thus, the major justifications for combining diagnostic quality CTD with PET would be to provide excellent anatomic image correlation in the cases, where subtle functional or lesion uptake requires greater localization refinement, and to reduce patient dose by removing the CTAC or CTAL exam in conjunction with a separate diagnostic CT in lieu of a single CTD exam. The choice of method depends on a variety of factors, including institutional and physician preference and experience, and technology availability.

**Keywords** CT · PET · Attenuation correction · CT optimization

## Background

The need for attenuation correction in positron emission tomography (PET) has been understood from the inception of the development of PET imaging. Attenuation correction for the $\gamma$-rays emitted from the positron annihilation is needed due to the high detection of scattered $\gamma$-rays and the loss of $\gamma$-rays due to attenuation from tissue and other material along the detection line of response (LOR). In PET imaging, 30–50% of the detected $\gamma$-rays in the main photopeak in the detection energy window consist of scattered photons, and the magnitude of attenuation correction is more pronounced in PET imaging (typical by a factor of $\sim 20$ compared to $\sim 6$ for [99 m-Tc] single-photon emission imaging) due to the need to image two-coincidental $\gamma$-ray photons traveling two separate antiparallel distances through the patient at a time over an extended imaging geometry [1–3]. Uncorrected attenuation losses from PET lead to increased image noise, distortions

✉ Samuel L. Brady
samuel.brady@stjude.org

Barry L. Shulkin
barry.shulkin@stjude.org

[1] Department of Diagnostic Imaging, St Jude Children's Research Hospital, 262 Danny Thomas Pl, Memphis, TN 38105, USA

in the image (such as from areas of high uptake or filling, e.g., urinary bladder), image artifacts, misrepresentation of uptake intensity (as seen along the skin surface due to a lack of attenuation effects compared to deeper in the body), and loss of quantitative accuracy. To account for the attenuation losses in the PET image, a means to develop an attenuation map, or $\mu$-map, is necessary. The $\mu$-map, once calculated, represents a spatial distribution of linear attenuation coefficients of the patient imaged and is applied to the raw PET image data at the time of PET reconstruction. The $\mu$-map serves to provide a mapping of attenuating material/tissue (based on their linear attenuation coefficients of that material/tissue) in the body and to compute an estimate of the scatter probability of the photons. To this end, various different approaches have been researched to provide attenuation correction for the PET image. Transmission imaging has largely been the most popular approach since the earliest days of emission tomography development [1].

In PET, transmission imaging is primarily tasked with correcting the degrading effects of annihilation photon attenuation from emission imaging, but it also provides anatomical co-localization of the emission and transmission data [2, 3]. From its inception, PET imaging focused largely on imaging the brain [4]. By the mid 1970s, with the introduction of the first ring geometry PET scanner, imaging with 2-deoxy-2-[18-F] fluoro-D-glucose ([18-F]-FDG) [5], and the introduction of a mechanized patient table that could insert the patient deeper into the PET scanner, PET imaging began to be developed for the whole body and not just the brain. Previously, attenuation correction for brain-only PET studies was largely a mathematical correction based on edge detection of the cranium [6]. The skull thickness and density were fairly consistent with patient size and only introduced small bias in the reconstructed PET image due to this variability. However, as PET studies began to cover the whole body, a need for more robust attenuation correction became essential due to larger-scale variability in patient body habitus [7].

Early in the evolution of PET, a [68Ge/68-Ga] rod or a [137-Cs] point source was used to acquire transmission scans through the patient to provide attenuation correction for the emitted positron radiation within the body [1–3, 8, 9]. The [68-Ge/68-Ga] source was the most commonly used source for acquisition of transmission data for attenuation correction [10]. For attenuation correction, initially, the [68-Ge/68-Ga] radionuclide was employed as a ring-shaped, rod-shaped, or point source-shaped transmission source, where the point source and rod were rotated near the surface of the scanner bore around the patient [11]. Three transmission scan methods using a radionuclide attenuation correction device were used over the years (Table 1). The first entailed performing the

transmission scan before the patient was injected with a radiotracer. This method eliminated the interference between the activity from the [68-Ge/68-Ga] transmission source and injected radiotracer, but was time consuming, because the patient had to remain on the scanner table during the radiotracer uptake (in the case of [18-F]-FDG, 45–60 min) and often suffered from transmission and emission co-registration errors from the patient moving during the uptake phase. The second and third methods entailed scanning the patient after the radiotracer was injected. The post-uptake transmission scan would either be acquired simultaneously during the emission scan, or after the emission scan was concluded. To overcome detector confusion from detecting the emission and transmission scan photons simultaneously [11], the scanner would track the location of the rod source position to know which detector block(s) were being exposed by the transmission rod. Two major limitations of these methods were (1) the count-rate performance of the detector and (2) length of time it took to acquire the transmission scan. First, the detector had to be able to handle the emission and transmission activities simultaneously. Second, due to the count-rate limitation of the PET detectors, transmission scanning with [68-Ge/68-Ga] rods took 2–10 min per bed position [1–3, 12].

Many of the transmission imaging limitations introduced by the [68-Ge/68-Ga] rod were overcome with the use of single-photon $\gamma$-ray point source, such as [137-Cs]. The [137-Cs] source was shielded on the side closest to the detector ring and rotated around the patient. Because the PET detectors on the opposite side of the gantry were the only ones accumulating transmission signal, and since there were not any random events to account for when counting single-photon events, the [137-Cs] could be a stronger transmission source, increasing the count rate by five to tenfold, thus decreasing noise in the transmission data and decreasing the time required to perform the transmission scan [9, 13]. Still, the use of [137-Cs] came with its limitations, namely: a 5–15% bias was introduced in the attenuation coefficient calculation due to the need to scale from a [137-Cs] photon energy of 662 keV to the positron annihilation energy 511 keV [13]. In addition, a minor increase in the fraction of cross-plane scatter photons came from the higher flux density from the [137-Cs] source, and since no co-linearity gate could be applied to the single $\gamma$-ray photon to reject the additional scatter.

In the early 1990s, low-cost PET configurations filled only a small subsection of the gantry with detector modules, and the PET gantry was rotated to produce the full PET image. Within the space between the PET detector modules, it was envisioned to place computed tomography (CT) scan equipment and use CT to acquire the transmission scan [14]. By 2000, a refined working model of a fully

**Table 1** Summary of transmission scan methods using a positron radionuclide (e.g., [68-Ge/68-Ga]) single-photon radionuclide (e.g., [137-Cs]) and CT for attenuation-corrected PET images

| Transmission scanning for PET attenuation correction | Pros | Cons |
| --- | --- | --- |
| Positron radionuclide transmission scan before radiotracer injection and uptake period | Eliminated interference between transmission and emission sources in the PET detector modules | Time consuming |
| | | Transmission and emission co-registration errors due to patient movement during uptake time |
| Positron radionuclide transmission and emission scanning performed simultaneously | Shortest scan time of the radionuclide transmission options | Count-rate performance limitation of PET detector due to the presence of emission and transmission photons |
| | | Transmission photons contributed to random and scatter coincidence events |
| Positron radionuclide transmission scan following complete emission scan | No additional contribution of randoms and scatter to coincidence events | Count-rate performance limitation of PET detector due to the presence of emission and transmission photons |
| | | Transmission scans took 2–10 min per bed position |
| Single-photon radionuclide transmission scan | Stronger transmission source lead to an increased (5–10 fold) flux density on the detector module | Attenuation correction bias due to mismatched photon energy with the 511 keV emission source data |
| | Decreased scan time | Slight increase in measured scatter events due to higher flux density |
| Computed tomography (CT) | CT detectors are independent of PET detectors and, therefore, are not count-rate limited | Attenuation correction bias due to mismatched photon energy with the 511 keV emission source data, and artifacts from transaxial scan FOV truncation, metallic implant, and anatomical motion mismatch |
| | Fast scan times | Increased patient dose compared to radionuclide methods |
| | Improved transmission scan image quality leads to greater PET image co-localization visibility | |
| | CT scanner can be used independently for diagnostic CT examinations | |

diagnostic hybrid PET/CT scanner was introduced [15]. By 2006, PET only scanners using radionuclide transmission sources were largely unobtainable for purchase, and were rapidly replaced by PET/CT. Though CT-based attenuation correction did not offer any improvement in the actual attenuation correction of the radionuclide image, as was shown by O'Conner et al. [16], CT did offer the advantage of high X-ray flux scanning obtained on dedicated X-ray detectors. Using CT for transmission scanning solved both the count-rate limitation from using PET detector modules, and the long transmission scan times of the radionuclide transmission scanning devices, since CT scanning is faster ($\sim$10 to 20 s total scan coverage) compared to the several minute per bed position radionuclide transmission scanning. In addition, since PET imaging has limited spatial resolution and limited visualization of anatomical landmarks [17], when combining PET and CT into one imaging modality, the CT component provides fast [10, 18] co-registration for anatomical localization in addition to attenuation correction for PET imaging [8].

Though PET/CT imaging has synergistic advantages over either component individually, and is the standard for PET imaging today, the use of CT has introduced several common artifacts, namely: (1) internal motion (major contributing factors: cardiac, respiratory, and bowel) caused misalignment between PET and CT; (2) truncation; (3) metallic implants; and (4) contrast medium [19]. Motion artifacts are the most prevalent artifact in PET/CT. (1) In general, the CT portion of the PET/CT exam is acquired with a form of breath hold (inspiration or expiration), thus obtained quickly without respiratory motion, whereas the PET portion of the PET/CT exam is acquired with free breathing, resulting in emission image anatomy averaged over many respiratory and cardiac cycles. The acquisition scheme mismatch often places CT anatomy, close to the lungs and heart, at different locations in the image than the PET imaged anatomy, thus leading to under or over attenuation correction of the radionuclide uptake (Fig. 1a). The most common example of this artifact is the lack of perceived radionuclide uptake in the shape of a curvilinear (or downward facing "banana") at the dome of the liver. (2) Truncation artifacts arise from the limited maximum field of view (FOV) of the CT scanner. If any portion of the patient anatomy resides outside the CT transaxial scan FOV (SFOV) during the CT scan, then the ability for the CT exam to provide attenuation correction for that anatomy is limited, and thus, the PET image reconstruction may be compromised (Fig. 1b). Some scanner manufacturers provide software corrections to mathematically account for
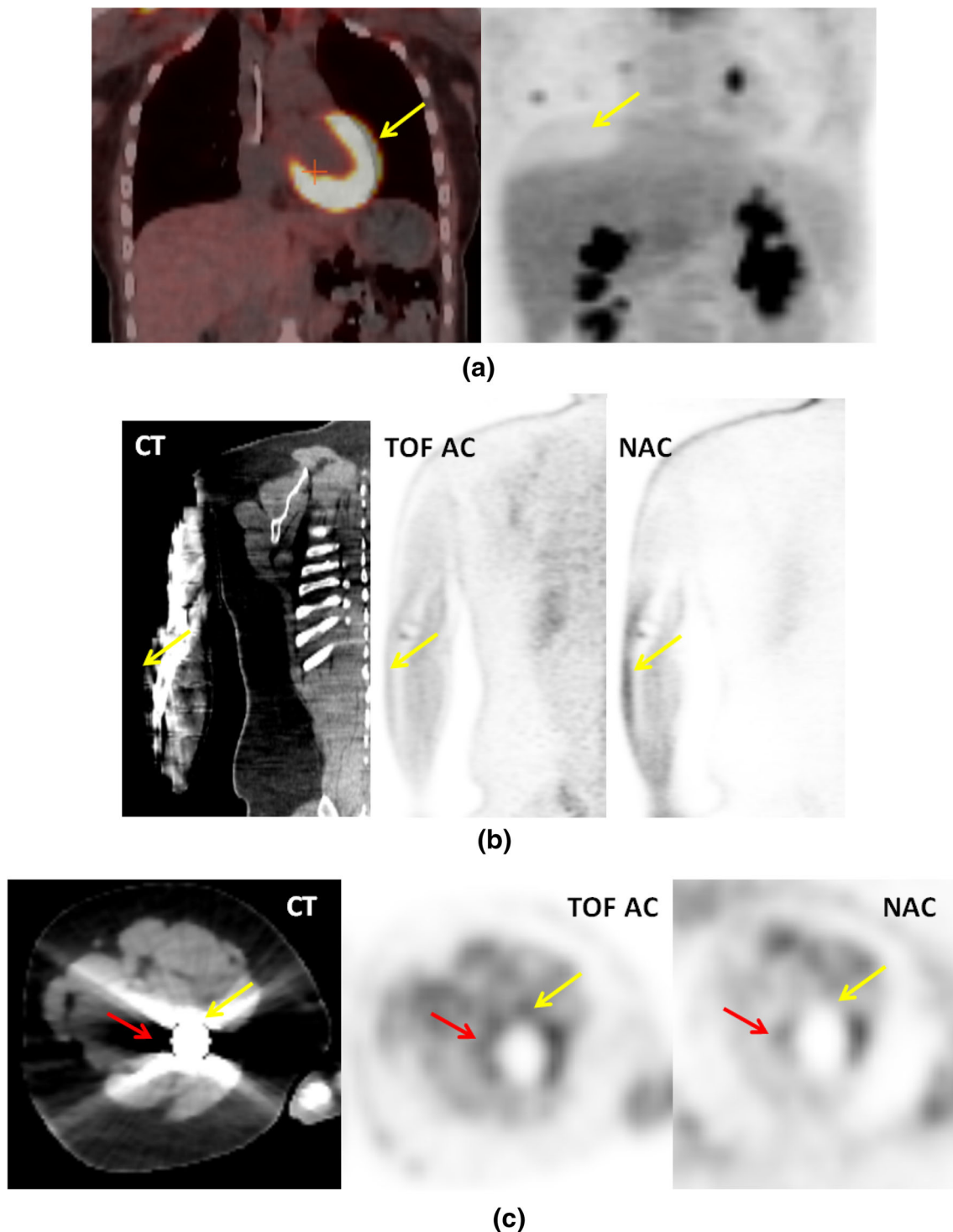
**(a)**



**(b)**



**(c)**

**Fig. 1 a** Internal motion caused artifacts generally manifest as a misalignment of CT anatomy and PET uptake in the heart (*left panel*) and at the dome of the liver (*right panel*). **b** Truncation artifacts occur when a portion of the patient's anatomy resides outside the CT transaxial SFOV (*left panel–right arm* clipped by CT SFOV causing sever CT artifacts). The ability for the CT to provide attenuation correction for that anatomy is limited (*central panel*—time of flight (TOF) attenuation correction [AC] and *right panel*—non-AC [NAC]).

**c** Metallic implants, such as left femur prosthesis, create CT artifacts in the form of streaking. The streaking artifacts lead to high CT numbers around the device (*left panel—yellow arrow*), which in turn may produce an overestimation of PET uptake (*central panel*—TOF AC *yellow arrow* compared to *right panel*—NAC *yellow arrow*). The lack of signal near a metallic device (*left panel–red arrow*) leads to an underestimation of uptake near the device (*central panel*—TOF AC *red arrow* compared to *right panel*—NAC *red arrow*)

truncation artifacts from attenuation losses in anatomy directly outside of the CT transaxial SFOV for PET attenuation correction. Such corrections have shown to improve attenuation reconstruction in PET to better than ∼5% as compared to the uncorrected SUV calculation of PET imaging without corresponding CT image outside the CT transaxial SFOV [20]. (3) Metallic implants, such as hip prosthesis, create CT artifacts in the form of streaking, which is due to a lack of signal due to photon starvation from lack of penetration of the metallic device(s). The streaking artifacts lead to high CT numbers around the device, which in turn may produce an overestimation of PET uptake. The lack of signal near a metallic device would have the opposite effect leading to an underestimation of uptake near the device (Fig. 1c). (4) Certain types of CT exams may require the injection of intravenous (IV) or ingestion of oral contrast agents. The purpose of contrast material is to provide visual contrast in the image, and help delineate anatomical structures that would otherwise have similar CT numbers and, therefore, similar grayscale appearance in the reconstructed image. Contrast material by nature is highly absorbent of photons and results in high CT numbers in the reconstructed image. When unaccounted for, these high CT numbers lead to erroneous $\mu$-map correction factors and over estimation of radionuclide uptake; however, it should be noted that the reconstruction software is used to mathematically account for high CT numbers from IV and oral contrast, and thus, contrast has been shown to be safe to use without adversely affecting PET attenuation correction or standard uptake value (SUV) quantitation [21–24].

Finally, with the combination of PET/CT imaging, so too is the radiation dose to the patient from both emission and transmission imaging components combined. CT X-ray flux density is on the order of 10 times [4] higher than isotope imaging sources, such as [68-Ge/68-Ga] rods [15]. A study by Wu et al. calculated an effective dose for a typical adult, and demonstrated that [68-Ge/68-Ga] transmission rods contributed an additional 0.2–0.3 mSv to the radionuclide PET study dose [10]. As a comparison, effective dose calculated for CT attenuation ranged from 7 to 43 mSv as reported in the past literature [10, 25–30]; the wide ranging effective dose levels varied largely on acquisition parameter selection, i.e., from dose reduced to fully diagnostic in quality, and demonstrates that no consensus has been achieved on how to acquire CT for attenuation correction. Various efforts to reduce CT radiation dose have been investigated, such as implementing automatic tube current modulation [31, 32], optimizing scan acquisition parameters (e.g., tube current, rotation time, and tube potential [18, 25, 33–36]), noise suppression methods to

allow the reduction of radiation output (i.e., tube current and tube potential) parameters while maintaining a defined reconstructed image quality (e.g., sinogram smoothing [37] or using iterative reconstruction [26, 38, 39]), and adding additional filtration [33]. Ultimately, CT acquisition parameters should be optimized based on the intended use of the CT for attenuation correction purposes.

## Introduction

The type of radiation dose optimization used for CT-based attenuation correction will largely depend on how the CT is utilized in conjunction with the PET image. Three broad categories have been suggested for the purpose of CT-based attenuation correction on the ImageWisely website [40]: (1) diagnosis; (2) anatomic localization of PET images; and (3) attenuation correction only for PET images; each approach to optimize the CT scan will provide the necessary attenuation correction information for full fidelity PET image formation. The three broad categories described on the ImageWisely website provide an opportunity for CT radiation dose adjustment depending on the purpose of the PET/CT study.

As was just described in Section I, the radionuclide transmission scan of the PET study was used for attenuation purposes only and did not provide a sufficient image quality to produce an image for more than gross anatomical localization [41] as can be seen in (Fig. 2a). In similar fashion, the acquisition of a CT exam for simple attenuation correction (CTAC) purposes of a PET/CTAC study should produce the lowest level of radiation dose possible for patient dose optimization. However, if anatomical co-localization of the PET and CT images along with attenuation correction is desired, an escalation in CT radiation dose, beyond CTAC level, would be required. In this scenario, the CT exam used for attenuation correction is not considered diagnostic but will provide the needed attenuation correction and CT image quality for anatomical localization (CTAL) for the PET/CTAL study [42]. Finally, when a diagnostic CT exam is ordered in conjunction with a PET/CT study, it may be possible, for patient dose optimization, to incorporate or replace the attenuation correction CT of the PET/CT study with the diagnostic CT exam and remove the redundant CT scan that would have been the CTAL or CTAC. Thus, the CT component of the study will be used for both attenuation correction and diagnostic purposes (CTD) and would be acquired using technique factors appropriate to produce a diagnostic CT exam in conjunction with the PET/CTD study [30, 42].
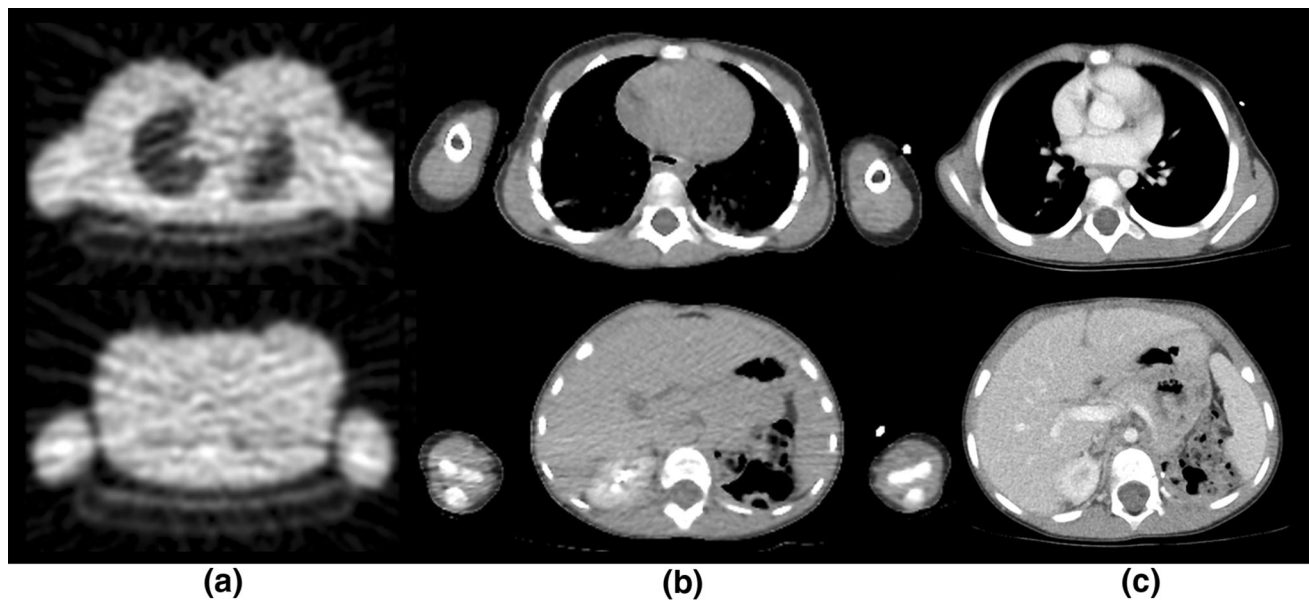
**Fig. 2** **a** Typical image quality of a radionuclide transmission scan of the chest and abdomen for attenuation correction purposes only. The images provided were acquired on a Siemens ECAT EXACT system using a [68-Ge/68-Ga] rotating rod source with approximately 2 min per bed position transmission scan time. **b** CTAL exam modified to be acquired using low-dose (0.8 mSv) acquisition technique factors (100 kVp, 10 mAs, and 1.0 mm in-plane pixel resolution) with the 100% iterative reconstruction software (ASiR; GE Healthcare). The images provided were acquired on a GE Discovery 690 system. **c** Typical diagnostic neck-chest-abdomen-pelvis CT exam using dose-reduced (2.4 mSv) diagnostic acquisition parameters (100 kVp, 38 mAs, and 0.6 mm in-plane pixel resolution) with IV and oral contrast administered. Images from **b** and **c** were acquired on the same day from the same patient, where image **c** was acquired first. A residual amount of contrast can be seen in the right kidney of image **b** due to excretion of recently administered IV contrast from image **c**

## Strategies for CT attenuation correction optimization

### CTAC for PET attenuation correction only

It has been demonstrated that when the CTAC is used for attenuation correction only, such as how the radionuclide sources were used in PET only devices that preceded the development of PET/CT, the radiation dose is lower, by approximately an order of magnitude, than typical low-dose CTAL exams [33, 37]. The primary limitation for implementation of the very low-dose CTAC only exams is the bias introduced into the PET reconstruction due to very noisy CT images. The noisy CT images are due to photon starvation at the detector due to low CT output from low tube current time product (mAs) and tube potential (kV) acquisition parameters and the presence of electronic noise in the CT electronic data acquisition systems (DAS). CT detectors are built to efficiently operate in the presence of high X-ray flux [43] due to the fact that the CT DAS does not energy discriminate and, therefore, was designed to integrate the inherently high flux density, polyenergetic spectrum of X-rays [43]. Low CT output leading to under correction of CT-based attenuation is primarily a limitation in adult PET/CT imaging for CT radiation dose reduction; moreover, for pediatric CT imaging, it was shown, in one

study [35], that radiation levels could be reduced by 100 fold and only introduce a noise bias in the PET reconstruction of 2%. The traditional radionuclide transmission attenuation correction was not bias-limited, because the PET detector DAS was designed for temporal and energy discrimination of detected photons and was thus better equipped to reject bias inducing scatter, single, and random events [43–45]; in addition, the radionuclides were of relatively lower photon count rate (even with the higher count rate of the single-photon γ-ray [137-Cs] source) compared to CT and the high penetrability of the [137-Cs] 611 keV and the [68-Ge/68-Ga] 511 keV γ-ray sources [33, 43]. To overcome the bias introduced into the PET reconstruction process from high-noise contaminated CTAC exams, sinogram smoothing [43], sparse sampling CT reconstruction with iterative reconstruction (such as model-based iterative reconstruction) [37], and added beam filtration [33] have been investigated and demonstrate good noise control for PET reconstruction bias on the order of only 5%.

With proposed noise limitation corrections for CT, Xia et al. [33] reported low-dose CT to vary between 0.14 and 0.42 mGy. Similarly, Fahey et al. [35] reported CTAC dose levels for pediatric exams between 0.3 and 0.42 mGy. Assuming a traditional eyes to thighs PET study, it is reasonable to assume comparable effective dose values,

i.e., 0.14–0.42 mSv based on an effective dose weighting factor ($w_T$) approximately equal to one. These low-dose CTAC estimated patient dose values are on the order of [68-Ge/68-Ga] transmission rod contributed radiation dose of 0.2–0.3 mSv [10].

Practical scenarios for application of PET/CTAC rely on the need for PET image data only for clinical diagnosis and no additional information provided from a visual interpretation of the CT. An example of this approach may be for the evaluation of the uptake and biodistribution of relatively long lived tracers, such as [89-Zr]-antibodies, that may require multiple imaging sessions over several days to determine the kinetics and optimal imaging times. A diagnostic PET/CTD or anatomical localization PET/CTAL could be obtained, followed by serial PET/CTAC for attenuation only in subsequent sessions to minimize dose exposure from the CT component of the examination. Another example would be for application of respiratory gated PET/CT. Respiratory gating supplies information about internal organ/tumor motion during a patient's breathing cycle. When tracking the respiratory motion of the patient using CT, the CT acquires a series of images corresponding to the PET axial position covering the diaphragm, over a period of time as to capture the full breathing cycle of the patient [46]. The CT scanner is either prospectively triggered to acquire an image at a particular phase of the respiratory cycle using a tracking device attached to the patient's body (either a passive system such as an infrared tracking marker placed on the skin surface [46, 47] or a pressure sensitive device placed around the patient's chest [47, 48]), or by acquiring a series of images covering the full respiratory cycle and retrospectively sorting the images based on the respiratory cycle trace measured using a tracking device. In one study [49], adult anthropomorphic phantom organ dose levels were measured based on typical CT acquisition parameters for respiratory gating; a mean effective dose of 33.1 mSv was calculated based on absolute organ dose values measured in the lungs, thyroids, breasts, and colon. If low-dose CTAC parameters were adopted as proposed by Fahey et al. [35] or Xia et al. [33] (i.e., 0.14–0.42 mGy) and compared to Matsuzaki et al. (i.e., 33.1 mGy), a potential radiation dose savings of 98% (0.42/33.1; mSv) to 99% (0.14/33.1; mSv) may potentially be possible for CT respiratory gating.

## CTAL for anatomic localization of CT and PET images

A more commonly found scenario for clinical prescription of a PET/CT examination is the acquisition of PET/CTAL with a sufficient CT image quality to provide anatomical localization between the CT and PET images, (Fig. 2b). In this common scenario, the radiation dose and other acquisition technique factors from the CT are elevated or enhanced to improve the quality of the image, but not to a level that would render the CT examination of a quality such to replace a diagnostic CT. Two items of consideration affecting the level of radiation output used for attenuation correction were used to define CT attenuation correction for anatomical localization or CTAL: first, the use of low tube current time product and tube potential technique parameters that do not bias the PET reconstruction and lead to accurate PET SUV quantification and second, a sufficient radiation output to limit quantum noise superimposition on the CT image [50].

First, studies have demonstrated CTAC radiation dose reductions by approximately 90%, from the standard CTD baseline dose levels, without introducing negative bias into pediatric PET reconstruction [25, 26, 35]. Substantial dose reduction can be applied for pediatric sized patients. For adult sized patients, the primary limitation to CTAL dose reduction was under correction of the CTAL-based attenuation correction from low kVp and low mAs scan techniques [18, 25, 26, 50]; in these studies, the CTAL acquisition technique was limited to 100–120 kVp and 35–65 mAs and produced dose reductions to 35–62% from a CTD dose.

The second investigation was that of the CTAL image quality and suitability for use of anatomical co-localization of the CT and PET image. At the reduced CTAL dose levels (∼90% for pediatric sized patients and 35–62% for medium-to-large sized adults), the appearance of the CT image is severely degraded and limits the ability for co-registered anatomical localization of [18-F]-FDG uptake in organs [50]. To preserve CT image quality, multiple different noise suppression and image quality preservation methods have been proposed. Xia et al. demonstrated with added filtration (0.5 mm Cu) and CT sinogram smoothing; at low-dose radiation output levels, CT and PET image quality is preserved [33, 43]. The use of iterative reconstruction for CT has been well documented to lower traditional CT radiation dose levels and maintains or improves diagnostic CT image quality [51–56]. Brady and Shulkin [26], Yang et al. [57], and Palmer and Fahey [58] investigated the use of adaptive statistical iterative reconstruction (ASiR; GE Healthcare), Rui et al. investigated the use of Model-based Iterative Reconstruction (VEO; GE, Healthcare) [37], and Tsa et al. investigated the use of Sinogram Affirmed Iterative Recon (SAFIRE, Siemens Medical) [59] to minimize noise infiltration in low-dose CTAL examinations for co-registered anatomical localization. Each study demonstrated image noise mitigation for the dose-reduced CTAL, accurate CT number reconstruction (i.e., no CT number bias leading to under correction of CT-based attenuation correction for PET reconstruction), and accurate PET SUV calculation. The

use of iterative reconstruction has allowed the implementation of dose-reduced CTAL acquisition while preserving appropriate CT image quality for anatomic co-localization between CT and PET images.

## CTD for CT attenuation correction, anatomical localization, and diagnostic analysis

Modern PET/CT systems combine into one system fully diagnostic CT scanning systems with the traditional full, multi-ring PET units, thus enabling the CT portion of the PET/CT exam to be acquired and interpreted in the same manner as any other diagnostic CT scan [60]. The benefits of implementing diagnostic quality CTD scanning for attenuation correction are that most PET/CT studies are ordered in tandem with a diagnostic CT scan as part of a clinical analysis for response to cancer therapy treatment, and the substitution of a diagnostic quality CT scan for the CTD portion of the PET/CTD provides potential radiation dose savings for the patient, potentially frees up clinical resources on a separate standalone diagnostic CT scanner that might otherwise be occupied performing a diagnostic CT on the PET patient, whose diagnostic CT could be provided as the PET/CTD, and provides high-quality CT images for anatomical co-localization with the reconstructed PET image. In order for the CTD to be considered diagnostic by definition, the scan must have the appropriate spatial resolution and image signal-to-noise ratio (SNR) [61] (Fig. 2c). To produce diagnostically acceptable spatial resolution for the clinical task at hand, beam collimation and the diameter of the area being imaged, or display FOV, should be appropriately set to provide correct pixel dimensions and reconstruction image magnification, where display FOV is established to accurately sample in-plane transaxial resolution, and beam collimation is established to accurately sample out-of-plane resolution along the main axis along the patient's body length. Image SNR is directly affected by establishing appropriate dose levels to allow diagnostic information to be obtained in low contrast regions that may be negatively impacted by image noise (i.e., quantum mottle) superimposed over the anatomical information [62]. Intravenous and oral contrast agents are often administered to improve image tissue differentiation in diagnostic CT exams (if no contraindications are present). The use of IV contrast in PET/CT may lead to enhanced lesion conspicuity in the CTD, where normal radiotracer, such as [18-F]-FDG, uptake, and accumulation, is known to be limited, and for oral contrast, to distend the bowel for increased conspicuity of luminal, mural, and extraluminal bowel disease and help distinguish physiologic from pathologic gastrointestinal uptake [21].

The disadvantage of combining PET and CTD is that the acquisition parameters for high-quality PET and CT exams have competing requirements that will require compromises to both CT and PET diagnostic image quality [42, 60]. Five competing acquisition parameters for PET/CTD are, first, the CT display FOV is a fixed acquisition parameter and cannot be decreased. The CT display FOV cannot be reduced for greater reconstruction magnification of smaller objects/patients required for diagnostic quality CT (e.g., the mapping of a smaller portion of the display FOV, such as the neck region, to the full $512 \times 512$ CT image matrix).

Second, image acquisition differences between diagnostic CT and PET led to discrepancies in contrast bolus injection timing schemes for multiphase contrast imaging. For diagnostic quality, CT requiring contrast enhancement, specific arterial, or venous contrast enhancement phases may require scan delays and scanning different scan series over different lengths of the patient's body in noncontiguous scanning schemes [21, 63]. Whereas for PET imaging, a single pass CT is generally acquired over the majority of the patient's body in one continuous motion (i.e., from the base of the skull through mid-femur) [63, 64]. If a single scan acquisition is acquired, contrast enhancement can appear muted or at best present as a mix of arterial and venous phase in the final reconstructed CT images rendering them non-diagnostic. If multiple scan series are prescribed in a traditional multiphase protocol, then misalignment between the CTD and PET data may occur due to the temporal mismatch of the CT and PET images from respiratory and cardiac motion, potential physical patient motion between the CT and PET scans, and physical misalignment due to potential repositioning of the patient arms [63]. Another limitation of the use of contrast agents is the formation of CT artifacts due to photonic starvation of the CT detectors. This limitation presents largely as a visual artifact when interpreting the CT image, and has been shown to not statistically effect the attenuation correction of the PET image, since strong smoothing filters are applied to the CT image that minimizes CT artifacts prior to PET reconstruction [67]. In addition, the patient may experience physiological effects from IV and/or oral contrast, such as nausea and vomiting that may lead to patient noncompliance and exam cancellation. In addition, most CT contrast media for IV contrast are hyperosmolar that may accelerate bladder filling during the PET acquisition, leading to patient discomfort, motion artifacts, and suboptimal evaluation of the pelvis. Minimizing the potentially limiting physiological effects from using contrast in a CTD would be to perform the CT component of the PET/CTD acquisition after the PET emission scan. However, this approach would cause delays in image reconstruction, as scanners generally begin processing images from a completed PET axial position, while images from the next axial position are being acquired.

This would effectively delay the image reconstruction until both the PET and CT acquisitions are complete, and not be ideal for busy clinics.

Third, diagnostic CT is generally acquired with a breath hold (either inspiration-for chest imaging or expiration-for abdominal imaging), whereas the traditional CTAC or CTAL imaging is acquired during free breathing or normal expiration breath hold and PET imaging is acquired during free breathing [19, 30, 42, 68]. As previously discussed, the difference between a full inspiration CTD and a free breathing PET acquisition may create spatial mis-registrations between the CT and PET images and potential attenuation correction inaccuracies [19]. Techniques to reduce respiration motion-induced artifacts are well established, but none of the established techniques are effective at mitigating the difference in spatial positioning of a full inspiration versus free breathing [68]. Most require a form of respiratory gating for both the CTD and PET exams. Introducing dynamic respiratory gating (or "4DCT") increases the imaging time for PET and the radiation dose from CT to the patient by $\sim 33$ mSv [49].

Fourth, diagnostic CT scan length is different than the traditional scan lengths needed for regular eyes to thighs or whole body PET/CTD scan lengths. As a dose-efficiency standard, diagnostic dose levels are used to scan the appropriate region of the body needed for diagnosis (e.g., lung apices to mid liver for chest-only). In an ideal setting when acquiring a PET/CTD, where the diagnostic CT order is for a chest-only (as an example), the CTD would comprise a standard or low-dose CTAC or CTAL starting at the beginning of the scan volume down to the point of the upper chest-only scan boundary (e.g., lung apices), where the scanner would then increase the radiation output to an appropriate level to acquire a diagnostic quality CT through the chest-only scan region followed by the remainder of the scan performed at standard or low-dose CTAC/CTAL. Most modern PET/CT scanners do not support a continuous motion dose-differential acquisition scheme as provided in the previous example. For a continuous motion CT, a typical PET/CT scanner would require diagnostic quality radiation levels over the whole of the CTD scan volume (i.e., eyes to thighs), thus, unnecessarily exposing sensitive organ systems to higher than needed radiation dose for attenuation correction purposes. For different CT series dose acquisition schemes, most modern PET/CT scanners can be programed to acquire separate CT scan series with different technique factors, as envisioned in the previous example; however, these scanners require inter-series scan delays that may introduce spatial misalignments, due to patient motion, between the various CT series and/or the whole CT series (spliced together) with the PET scan. Typical inter-series scan delays are due to the scanner needing time to adjust technique factors (i.e., tube potential, rotation speed, etc.), and reposition the patient table (in the case of helical acquisition which needs to acquire extra scan volume before and after the programed CT series start and stop locations, i.e., "over-ranging") [69].

Finally, in most cases, patient arm positioning for diagnostic CT of the body is conducted with arms above the patient's head to remove beam hardening artifacts that would manifest as streaks through the scanned volume. However, in PET imaging, the patient's arms are generally placed along the patient's side; thus, any streak artifacts produced, because the arms in the transaxial SFOV may compromise CT imaging of the thorax and upper abdomen. Similarly, if arms were placed above the head, the potential streak artifacts would impact imaging of the head and neck regions [19, 67, 70]. Options as to where the patient arms can be placed for the duration of the PET/CT exam (which can last upwards of 15–45 min) may be limited due to patient compliance (i.e., comfort) [67, 70, 71] and medical device access (e.g., in the case, where general anesthesia is administered, arm placement is dependent on accessing the arm for drug administration, etc.). In addition, when the arms are placed either above, or below the patient's head, if the arms are not fully included in the transaxial SFOV, truncation artifacts will occur and have been shown to degrade both the CT and PET image quality [20]. It has been recommended that patient arms should be placed in a comfortable location for the duration of the exam, and when the arms are to be included in the PET diagnosis, they should be placed fully within the transaxial SFOV, but in a position as not to affect the CT or PET diagnostic image quality [70]. When the patient arms need to be placed at their side, the use of different arm pillows and sponges to elevate the arms at an approximate 45° may allow the patient to maintain the arms at their side for comfort/compliance while minimizing the beam hardening streak artifacts in the throrax and abdomen regions of the images without affecting reconstructed image quality.

When considering the compromises required for the acquisition of PET/CTD, customization of specific protocols has been suggested that would require a separate diagnostic CT and PET with low-dose CTAC or CTAL for the initial disease staging, and then allow for PET/CTD exams for follow-up [60]. In addition, when imaging for a particular disease, such as lymphoma [72] or melanoma [60], it has been suggested that PET/noncontrast-CTAL removes the need for additional diagnostic contrast-enhanced CTD.

## Current and future trends in CT dose optimization

The current and future methods for reducing patient dose from CT have been largely technology driven. Siemens has introduced technology to only scan the required volume prescribed by the supervising physician or technologist by

introducing continuous motion PET/CT. The current CT scanners are required to acquire CT imaging over the full volume of the PET axial position (which may run between 16 and 18 cm along the patient's z-axis). Recent technology has been implemented to allow for variable, continuous table motion (FlowMotion, Siemens Medical) instead of a traditional step and shoot acquisition. Continuous table motion allows more flexible prescription of the volume eliminating potential over scanning of patient anatomy outside of the prescribed scan range. The ability to vary the table speed allows for optimization of image quality over areas of the body requiring higher resolution (i.e., slower table motion for better image quality) and to go faster over areas not requiring the same level of image quality [73]. In addition, the continuous motion technology has been shown to improve the clinical workflow efficiency of respiratory gating [73].

In another technology, GE has introduced a very low-dose CT, on the order of CTAC at 0.3–0.62 mSv, but with image quality sufficient for anatomical localization (Q.AC, GE Healthcare) [74]. The higher image quality low-dose CTAC is made possible through a variety of factors: more sensitive CT detectors (able to produce greater light scintillation per X-ray photon, which leads to less signal noise for a better image reconstruction), lower dose acquisition parameters (X-ray generator that can operate at lower technique factors), and new iterative reconstruction techniques. The new Q.AC allows for low-dose attenuation correction and respiratory gating. Similarly, Toshiba has introduced iterative reconstruction (AIDR 3D), for enhanced CT noise control in reconstruction—allowing for low-dose acquisition techniques, and a wide detector, 32 slice, CT for greater dose efficiency.

Other approaches for CT dose mitigation seek to use emission data only, such as from time of flight (TOF), to provide attenuation correction [75], and the use of non-ionizing techniques to acquire transmission attenuation correction of PET data in a PET/MRI [76–81]. With the introduction of PET/MRI, attenuation correction for PET reconstruction could not be handled using the traditional methods. Since transmission and CT-based techniques are incompatible with PET/MRI geometries and physical constraints (such as being immersed within a strong magnetic field), the use of MRI acquisition techniques, such as the Dixon-VIBE method, direct segmentation with or without atlases, and templates [82], are routinely used; such methods provide to the patient inherent radiation dose sparing from what would have been a CT attenuation correction acquisition. In addition, with the adoption of PET/MRI, it has been demonstrated that overall PET injected dose levels may be reduced substantially due, in part, to the longer dwell time required for each PET axial position to acquire the MRI sequence(s) prescribed with the PET scan [83].

Due to the unique challenges that come from providing attenuation correction data for PET imaging within an MRI environment, research into alternative methods for PET attenuation correction has been investigated. Recently, Defrise et al. [84] demonstrated that TOF PET data contain within the emission sinogram all values necessary to estimate the attenuation and the activity information to reconstruct a PET image. From this study [84], an analytical method demonstrated a unique solution (except for a constant that can be estimated efficiently) to the mathematical construct that establishes, from the available TOF information, the estimation of attenuation and activity. The authors suggest that the TOF analytical method, combined with Poissonian noise modeling and iterative algorithms, may provide a future framework for direct, simultaneous reconstruction of emission and attenuation data.

## Summary

Advances in CT technology have provided opportunities to acquire CT for attenuation correction in a variety of ways, allowing for the optimization of the CT for specific clinical purposes, such as PET/CTAC, PET/CTAL, or PET/CTD. Table 2 provides a summary list of acquisition parameters and typical delivered radiation doses for these three optimization approaches as found in the scientific literature.

Some institutions obtain PET/CTD only, while others obtain PET/CTAL for localization only, followed or preceded by diagnostic quality CT restricted to a particular

**Table 2** Following is a compilation of published CT exam technique factors and their typical radiation dose levels

| Optimization type | kVp | mAs | Pitch | Effective dose (mSv) | References |
|---|---|---|---|---|---|
| CTAC | 80 | 0.25 | | 0.42 | Xia et al. [33] |
| CTAC | 80 | 5 | 1.5 | 0.42 | Fahey et al. [35] |
| CTAC | 120 | 5 | 1.5 | 0.64 | Fahey et al. [35] |
| CTAL | 80–120 | 10–25 | 0.98 | 0.9–3.2 | Brady, Shulkin [26] |
| CTAL | 120–140 | 10–40 | 1–1.5 | 2.1–4.6 | Fahey [18] |
| CTAL | 120 | 10–40 | 0.98 | 2.9–6.3 | Alessio et al. [25] |
| CTD | 120–140 | 111–200 | 1–1.25 | 14.1–18.6 | Brix et al. [27] |

section of the body. With modern dose reduction techniques for CTAL, and some technological advances allowing CTAC exams to have a sufficient image quality for anatomical localization, the additional radiation exposure from a non-diagnostic CT attenuation correction exam is low. Thus, the major justifications for combining diagnostic quality CT as CTD (understanding the challenges described previously of acquiring a truly diagnostic CT during a CTD) would be to provide excellent anatomic image correlation capabilities for PET images, in the cases, where subtle functional or lesion uptake requires greater localization refinement, and to reduce patient dose by removing the CTAC or CTAL exam in conjunction with a separate diagnostic CT in lieu of a single CTD exam.

ImageWisely has recommended three broad categories for the dose optimization of CT for attenuation correction purposes in PET/CT imaging: (1) CTD for fully diagnostic CT quality; (2) CTAL for anatomic localization of PET images; and (3) CTAC for PET attenuation correction only. All three categories were discussed in this review along with an analysis and discussion of the estimated patient dose levels for each category.

# References

1. Bailey DL (1998) Transmission scanning in emission tomography. Eur J Nucl Med 25:774–787
2. Zaidi H, Hasegawa B (2003) Determination of the attenuation map in emission tomography. J Nucl Med 44:291–315
3. Kinahan PE, Hasegawa BH, Beyer T (2003) X-ray-based attenuation correction for positron emission tomography/computed tomography scanners. Semin Nucl Med 33:166–179
4. Portnow LH, Vaillancourt DE, Okun MS (2013) The history of cerebral PET scanning: from physiology to cutting-edge technology. Neurology 80:952–956
5. Nutt R (2002) The history of positron emission tomography. Mol Imag Biol 4:11–26
6. Bergstrom M, Litton J, Eriksson L, Bohm C, Blomqvist G (1982) Determination of object contour from projections for attenuation correction in cranial positron emission tomography. J Comput Assist Tomogr 6:365–372
7. Carson RE, Daube-Witherspoon ME, Green MV (1988) A method for postinjection PET transmission measurements with a rotating source. J Nucl Med 29:1558–1567
8. Kinahan PE, Townsend DW, Beyer T, Sashin D (1998) Attenuation correction for a combined 3D PET/CT scanner. Med Phys 25:2046–2053
9. Karp JS, Muehllehner G, Qu H, Yan XH (1995) Singles transmission in volume-imaging PET with a 137Cs source. Phys Med Biol 40:929–944
10. Wu TH, Huang YH, Lee JJ, Wang SY, Wang SC, Su CT, Chen LK, Chu TC (2004) Radiation exposure during transmission measurements: comparison between CT- and germanium-based techniques with a current PET scanner. Eur J Nucl Med Mol Imaging 31:38–43
11. Ostertag H, Kubler WK, Doll J, Lorenz WJ (1989) Measured attenuation correction methods. Eur J Nucl Med 15:722–726
12. Bacharach SL (2007) PET/CT attenuation correction: breathing lessons. J Nucl Med 48:677–679
13. deKemp RA, Nahmias C (1994) Attenuation correction in PET using single photon transmission measurement. Med Phys 21:771–778
14. Townsend DW (2008) Combined positron emission tomography-computed tomography: the historical perspective. Semin Ultrasound CT MR 29:232–235
15. Beyer T, Townsend DW, Brun T, Kinahan PE, Charron M, Roddy R, Jerin J, Young J, Byars L, Nutt R (2000) A combined PET/CT scanner for clinical oncology. J Nucl Med 41:1369–1379
16. O'Connor MK, Kemp BJ (2006) Single-photon emission computed tomography/computed tomography: basic instrumentation and innovations. Semin Nucl Med 36:258–266
17. Brix G, Lechel U, Glatting G, Ziegler SI, Munzing W, Muller SP, Beyer T (2005) Radiation exposure of patients undergoing whole-body dual-modality 18F-FDG PET/CT examinations. J Nucl Med 46:608–613
18. Fahey FH (2009) Dosimetry of pediatric PET/CT. J Nucl Med 50:1483–1491
19. Sureshbabu W, Mawlawi O (2005) PET/CT imaging artifacts. J Nucl Med Technol 33:156–161
20. Mawlawi O, Erasmus JJ, Pan T, Cody DD, Campbell R, Lonn AH, Kohlmyer S, Macapinlac HA, Podoloff DA (2006) Truncation artifact on PET/CT: impact on measurements of activity concentration and assessment of a correction algorithm. AJR Am J Roentgenol 186:1458–1467
21. Antoch G, Freudenberg LS, Beyer T, Bockisch A, Debatin JF (2004) To enhance or not to enhance? 18F-FDG and CT contrast agents in dual-modality 18F-FDG PET/CT. J Nucl Med 45(Suppl 1):56S–65S
22. Berthelsen AK, Holm S, Loft A, Klausen TL, Andersen F, Hojgaard L (2005) PET/CT with intravenous contrast can be used for PET attenuation correction in cancer patients. Eur J Nucl Med Mol Imaging 32:1167–1175
23. Cronin CG, Prakash P, Blake MA (2010) Oral and IV contrast agents for the CT portion of PET/CT. AJR Am J Roentgenol 195:W5–W13
24. Yau YY, Chan WS, Tam YM, Vernon P, Wong S, Coel M, Chu SK (2005) Application of intravenous contrast in PET/CT: does it really introduce significant attenuation correction error? J Nucl Med 46:283–291
25. Alessio AM, Kinahan PE, Manchanda V, Ghioni V, Aldape L, Parisi MT (2009) Weight-based, low-dose pediatric whole-body PET/CT protocols. J Nucl Med 50:1570–1577
26. Brady SL, Shulkin BL (2015) Ultralow dose computed tomography attenuation correction for pediatric PET CT using adaptive statistical iterative reconstruction. Med Phys 42:558–566
27. Brix G, Lechel U, Glatting G, Ziegler SI, Munzing W, Muller SP, Beyer T (2005) Radiation exposure of patients undergoing whole-body dual-modality 18F-FDG PET/CT examinations. J Nucl Med 46:608–613
28. Huang B, Law MW, Khong PL (2009) Whole-body PET/CT scanning: estimation of radiation dose and cancer risk. Radiology 251:166–174
29. NCRP (2009) NCRP Report No 160: ionizing radiation exposure of the population of the United States, pp 1–387
30. Boellaard R, O'Doherty MJ, Weber WA, Mottaghy FM, Lonsdale MN, Stroobants SG, Oyen WJ, Kotzerke J, Hoekstra OS, Pruim J, Marsden PK, Tatsch K, Hoekstra CJ, Visser EP, Arends B, Verzijlbergen FJ, Zijlstra JM, Comans EF, Lammertsma AA, Paans AM, Willemsen AT, Beyer T, Bockisch A, Schaefer-Prokop C, Delbeke D, Baum RP, Chiti A, Krause BJ (2010) FDG PET and PET/CT: EANM procedure guidelines for tumour PET imaging: version 1.0. Eur J Nucl Med Mol Imaging 37:181–200

31. Kamel E, Hany TF, Burger C, Treyer V, Lonn AH, von Schulthess GK, Buck A (2002) CT vs 68Ge attenuation correction in a combined PET/CT system: evaluation of the effect of lowering the CT tube current. Eur J Nucl Medicine Mol Imaging 29:346–350

32. Jackson J, Pan T, Tonkopi E, Swanston N, Macapinlac HA, Rohren EM (2011) Implementation of automated tube current modulation in PET/CT: prospective selection of a noise index and retrospective patient analysis to ensure image quality. J Nucl Med Technol 39:83–90

33. Xia T, Alessio AM, De Man B, Manjeshwar R, Asma E, Kinahan PE (2012) Ultra-low dose CT attenuation correction for PET/CT. Phys Med Biol 57:309–328

34. Yu L, Li H, Fletcher JG, McCollough CH (2010) Automatic selection of tube potential for radiation dose reduction in CT: a general strategy. Med Phys 37:234–243

35. Fahey FH, Palmer MR, Strauss KJ, Zimmerman RE, Badawi RD, Treves ST (2007) Dosimetry and adequacy of CT-based attenuation correction for pediatric PET: phantom study. Radiology 243:96–104

36. Mattsson S, Andersson M, Soderberg M (2015) Technological advances in hybrid imaging and impact on dose. Radiat Prot Dosim 165:410–415

37. Rui X, Cheng L, Long Y, Fu L, Alessio AM, Asma E, Kinahan PE, De Man B (2015) Ultra-low dose CT attenuation correction for PET/CT: analysis of sparse view data acquisition and reconstruction algorithms. Phys Med Biol 60:7437–7460

38. Matsutomo N, Nagaki A, Sasaki M (2015) Validation of the CT iterative reconstruction technique for low-dose CT attenuation correction for improving the quality of PET images in an obesity-simulating body phantom and clinical study. Nucl Med Commun 36:839–847

39. De Man B, Nuyts J, Dupont P, Marchal G, Suetens P (2001) An iterative maximum-likelihood polychromatic algorithm for CT. IEEE Trans Med Imaging 20:999–1008

40. Alessio AM, Kinahan PE. CT protocol selection in PET-CT imaging," (ImageWisely.org, http://www.imagewisely.org/~/media/ImageWisely-Files/NucMed/CT-Protocol-Selection-in-PET-CT-Imaging.pdf, 2012)

41. Alessio AM, Kinahan PE, Cheng PM, Vesselle H, Karp JS (2004) PET/CT scanner instrumentation, challenges, and solutions. Radiol Clin North Am 42:1017–1032

42. Delbeke D, Coleman RE, Guiberteau MJ, Brown ML, Royal HD, Siegel BA, Townsend DW, Berland LL, Parker JA, Hubner K, Stabin MG, Zubal G, Kachelriess M, Cronin V, Holbrook S (2006) Procedure guideline for tumor imaging with 18F-FDG PET/CT 1.0. J Nucl Med 47:885–895

43. Xia T, Alessio AM, Kinahan PE(2010) Limits of ultra-low dose CT attenuation correction for PET/CT. In: IEEE Nuclear Science Symposium Conference Record, vol 1997: pp 3074–3079

44. Lecomte R (2009) Novel detector technology for clinical PET. Eur J Nucl Med Mol Imaging 36(Suppl 1):S69–S85

45. Budinger TF (1998) PET instrumentation: what are the limits? Semin Nucl Med 28:247–267

46. Nehmeh SA, Erdi YE, Rosenzweig KE, Schoder H, Larson SM, Squire OD, Humm JL (2003) Reduction of respiratory motion artifacts in PET imaging of lung cancer by respiratory correlated dynamic PET: methodology and comparison with respiratory gated PET. J Nucl Med 44:1644–1648

47. Callahan J, Kron T, Schneider-Kolsky M, Hicks RJ (2011) The clinical significance and management of lesion motion due to respiration during PET/CT scanning. Cancer Imaging 11:224–236

48. Hope TA, Verdin EF, Bergsland EK, Ohliger MA, Corvera CU, Nakakura EK (2015) Correcting for respiratory motion in liver PET/MRI: preliminary evaluation of the utility of bellows and navigated hepatobiliary phase imaging. EJNMMI Phys 2:21

49. Matsuzaki Y, Fujii K, Kumagai M, Tsuruoka I, Mori S (2013) Effective and organ doses using helical 4DCT for thoracic and abdominal therapies. J Radiat Res 54:962–970

50. Krishnasetty V, Bonab AA, Fischman AJ, Halpern EF, Aquino SL (2008) Comparison of standard-dose vs low-dose attenuation correction CT on image quality and positron emission tomographic attenuation correction. J Am Coll Radiol 5:579–584

51. Brady S, Moore B, Yee B, Kaufman R (2014) Implementation of ASiR™ reconstruction for substantial dose reduction in pediatric CT without affecting image noise. Radiology 270:223–231

52. Brady SL, Yee BS, Kaufman RA (2012) Characterization of adaptive statistical iterative reconstruction algorithm for dose reduction in CT: a pediatric oncology perspective. Med Phys 39:5520–5531

53. Hara AK, Paden RG, Silva AC, Kujak JL, Lawder HJ, Pavlicek W (2009) Iterative reconstruction technique for reducing body radiation dose at CT: feasibility study. AJR Am J Roentgenol 193:764–771

54. Prakash P, Kalra MK, Digumarthy SR, Hsieh J, Pien H, Singh S, Gilman MD, Shepard JA (2010) Radiation dose reduction with chest computed tomography using adaptive statistical iterative reconstruction technique: initial experience. J Comput Assist Tomogr 34:40–45

55. Silva AC, Lawder HJ, Hara A, Kujak J, Pavlicek W (2010) Innovations in CT dose reduction strategy: application of the adaptive statistical iterative reconstruction algorithm. AJR Am J Roentgenol 194:191–199

56. Singh S, Kalra MK, Gilman MD, Hsieh J, Pien HH, Digumarthy SR, Shepard JA (2011) Adaptive statistical iterative reconstruction technique for radiation dose reduction in chest CT: a pilot study. Radiology 259:565–573

57. Yang B-H, Wu N-Y, Chen G-L, Wu T-H (2016) The optimal protocols of low-dose CT with iterative reconstruction CT in PET/CT scan. J Nucl Med 57:2675

58. Palmer MR, Fahey FH (2012) Attenuation correction in PET/CT from ultra-low dose CT: photon starvation and iterative CT reconstruction. J Nucl Med 53:2360

59. Fa-Shun Tsa S-C, Wang H-H, Chou T-L, Jiang L-COu (2014) SAFIRE improves CT image quality in PET/CT scans: An ACR CT phantom test. Ann Nucl Med Mol Imaging 27:3–11

60. Wong TZ, Paulson EK, Nelson RC, Patz EF Jr, Coleman RE (2007) Practical approach to diagnostic CT combined with PET. AJR Am J Roentgenol 188:622–629

61. Kuehl H, Veit P, Rosenbaum SJ, Bockisch A, Antoch G (2007) Can PET/CT replace separate diagnostic CT for cancer imaging? Optimizing CT protocols for imaging cancers of the chest and abdomen. J Nucl Med 48(Suppl 1):45S–57S

62. Gollub MJ, Hong R, Sarasohn DM, Akhurst T (2007) Limitations of CT during PET/CT. J Nucl Med 48:1583–1591

63. Brechtel K, Klein M, Vogel M, Mueller M, Aschoff P, Beyer T, Eschmann SM, Bares R, Claussen CD, Pfannenberg AC (2006) Optimized contrast-enhanced CT protocols for diagnostic whole-body 18F-FDG PET/CT: technical aspects of single-phase versus multiphase CT imaging. J Nucl Med 47:470–476

64. Beyer T, Antoch G, Bockisch A, Stattaus J (2005) Optimized intravenous contrast administration for diagnostic whole-body 18F-FDG PET/CT. J Nucl Med 46:429–435

65. Nakamoto Y, Chin BB, Kraitchman DL, Lawler LP, Marshall LT, Wahl RL (2003) Effects of nonionic intravenous contrast agents at PET/CT imaging: phantom and canine studies. Radiology 227:817–824

66. Joshi U, Raijmakers PG, Riphagen II, Teule GJ, van Lingen A, Hoekstra OS (2007) Attenuation-corrected vs. nonattenuation-corrected 2-deoxy-2-[F-18]fluoro-d-glucose-positron emission

tomography in oncology: a systematic review. Mol Imaging Biol 9:99–105

67. Blodgett TM, Mehta AS, Mehta AS, Laymon CM, Carney J, Townsend DW (2011) PET/CT artifacts. Clin Imaging 35:49–63

68. Sun T, Mok GS (2012) Techniques for respiration-induced artifacts reductions in thoracic PET/CT. Quant Imaging Med Surg 2:46–52

69. Schilham A, van der Molen AJ, Prokop M, de Jong HW (2010) Overranging at multisection CT: an underestimated source of excess radiation exposure. Radiographics 30:1057–1067

70. Boellaard R, Delgado-Bolton R, Oyen WJ, Giammarile F, Tatsch K, Eschner W, Verzijlbergen FJ, Barrington SF, Pike LC, Weber WA, Stroobants S, Delbeke D, Donohoe KJ, Holbrook S, Graham MM, Testanera G, Hoekstra OS, Zijlstra J, Visser E, Hoekstra CJ, Pruim J, Willemsen A, Arends B, Kotzerke J, Bockisch A, Beyer T, Chiti A, Krause BJ, European Association of Nuclear M (2015) FDG PET/CT: EANM procedure guidelines for tumour imaging: version 2.0. Eur J Nucl Med Mol Imaging 42:328–354

71. Beyer T, Antoch G, Muller S, Egelhof T, Freudenberg LS, Debatin J, Bockisch A (2004) Acquisition protocol considerations for combined PET/CT imaging. J Nucl Med 45(Suppl 1):25S–35S

72. Elstrom RL, Leonard JP, Coleman M, Brown RK (2008) Combined PET and low-dose, noncontrast CT scanning obviates the need for additional diagnostic contrast-enhanced CT scans in patients undergoing staging or restaging for lymphoma. Ann Oncol 19:1770–1773

73. Acuff S, Osborne DR (2016) Clinical workflow considerations for implementation of continuous bed motion PET/CT. J Nucl Med Technol 44:55–58. doi:10.2967/jnmt.116.172171

74. Jeong SW, Kim HG, Gwon JB, Shin YM, Kim YH (2014) Effect of the dose reduction applied low dose for PET/CT according to CT attenuation correction method. J Nucl Med 55:2635

75. Berker Y, Li Y (2016) Attenuation correction in emission tomography using the emission data—a review. Med Phys 43:807–832

76. Daftary A (2010) PET-MRI: challenges and new directions. Indian J Nucl Med 25:3–5

77. Judenhofer MS, Wehrl HF, Newport DF, Catana C, Siegel SB, Becker M, Thielscher A, Kneilling M, Lichy MP, Eichner M, Klingel K, Reischl G, Widmaier S, Rocken M, Nutt RE, Machulla HJ, Uludag K, Cherry SR, Claussen CD, Pichler BJ (2008) Simultaneous PET-MRI: a new approach for functional and morphological imaging. Nat Med 14:459–465

78. Pichler BJ, Kolb A, Nagele T, Schlemmer HP (2010) PET/MRI: paving the way for the next generation of clinical multimodality imaging applications. J Nucl Med 51:333–336

79. Spick C, Herrmann K, Czernin J (2016) 18F-FDG PET/CT and PET/MRI perform equally well in cancer: evidence from studies on more than 2300 patients. J Nucl Med 57:420–430

80. Zaidi H, Becker M (2016) The Promise of Hybrid PET/MRI: technical advances and clinical applications. IEEE Signal Process Mag 33:67–85

81. Vogelius E, Shah S (2017) Pediatric PET/MRI: a review. J Am Osteopath Coll Radiol 6:15–27

82. Wagenknecht G, Kaiser HJ, Mottaghy FM, Herzog H (2013) MRI for attenuation correction in PET: methods and challenges. Magma 26:99–113

83. Schafer JF, Gatidis S, Schmidt H, Guckel B, Bezrukov I, Pfannenberg CA, Reimold M, Ebinger M, Fuchs J, Claussen CD, Schwenzer NF (2014) Simultaneous whole-body PET/MR imaging in comparison to PET/CT in pediatric oncology: initial results. Radiology 273:220–231

84. Defrise M, Rezaei A, Nuyts J (2012) Time-of-flight PET data determine the attenuation sinogram up to a constant. Phys Med Biol 57:885–899